JOURNAL OF MATERIALS SCIENCE 27 (1992) 761–766

Cooling and solidification of liquid-metal drops in a gaseous atmosphere

J. K. McCOY, A. J. MARKWORTH, E. W. COLLINGS
Battelle, 505 King Avenue, Columbus, Ohio 43201, USA
R. S. BRODKEY
Ohio State University, Columbus, Ohio 43210, USA

The free fall of a liquid-metal drop, heat transfer from the drop to its environment, and solidification of the drop are described for both gaseous and vacuum atmospheres. A simple model, in which the drop is assumed to fall rectilinearly, with behaviour like that of a rigid particle, is developed to describe cooling behaviour. Recalescence of supercooled drops is assumed to occur instantaneously when a specified temperature is passed. The effects of solidification and experimental parameters on drop cooling are calculated and discussed. Major results include temperature as a function of time, and of drag, time to complete solidification, and drag as a function of the fraction of the drop solidified.

1. Introduction

The usefulness of drop tubes for studies of containerless liquid-metal supercooling is well established [1–4]. The typical experiment involves a small (several millimetres in diameter) drop falling from a levitated position within an evacuated or helium-filled drop tube chamber. The atmosphere provides added heat transfer capabilities, but also results in a drag force on the drop that can affect its motion.

Modelling studies of liquid-drop kinematics during the several second fall period, as well as of related processes, such as internal circulation and heat transfer, must be carried out to both guide and interpret corresponding experimental studies. Accordingly, several such studies have been reported [1, 2, 5].

The work presented here consists of another modelling study, the distinguishing features of which include more general treatments of such factors as the drag force and convective heat transfer as well as treatment of supercooling and solidification. Application of the model is made to a number of pure metal systems, which leads to considerable insight into expected drop behaviour and hence to suggested experimental studies.

2. Differential equations for a falling drop

In this section, we briefly develop the differential equations for a falling drop. A more detailed discussion, including justification for the various approximations, has been published previously [6].

The differential equations of motion for the drop are

$$dx/dt = U \quad (1)$$

$$dU/dt = g\Delta\rho/\rho_p - 3C_d\rho U^2/4\rho_p d \quad (2)$$

where g is the gravitational field strength, ρ is the density of the gas, ρ_p is the density of the drop, $\Delta\rho = \rho_p - \rho$, C_d is the coefficient of drag, d is the drop diameter, U is the drop speed, x is the distance fallen, and t is time. The drag coefficient, C_d, depends on the Reynolds number (Re); we used the steady state drag correlations for spheres recommended by Clift, Grace and Weber [7], which are applicable at low Mach and Knudsen numbers.

The differential equation for heat transfer is

$$dT_p/dt = [-\varepsilon s(T_p^4 - T^4) - h(T_p - T)](6/C_p\rho_p d) \quad (3)$$

where T_p is the drop temperature, ε is the emittance, s is the Stefan–Boltzmann constant, h is the heat transfer coefficient, and C_p is the heat capacity of the metal. In using Equation 3, it is assumed that there are no temperature gradients within the drop, that no phase changes occur, and that the temperature of the gas far from the drop and the mean radiative temperature of the environment are both T.

In our calculations, Equations 1–3 were solved numerically by a non-adaptive fourth order Runge–Kutta method [8]. Although this is a simple method, it provides sufficient accuracy. For the calculations reported here, we found that the global error due to the numerical integration is less than 0.06 K for temperature and less than 1.2 mm for position.

The results reported were obtained with the White model of heat transfer [9]

$$h = (K_t/d)(2 + 0.3\mathrm{Pr}^{1/3}\mathrm{Re}^{0.6}) \quad (\mathrm{Re} < 100000) \quad (4)$$

where Pr is the Prandtl number of the gas, K_t is the thermal conductivity of the gas, and d is the drop

0022–2461/92 $03.00 + .12 © *1992 Chapman & Hall*

diameter. In this model, gas properties are evaluated at the film temperature T_f,

$$T_f = (T + T_p)/2 \quad (5)$$

3. Thermophysical properties

Thermophysical properties of the drops were collected from a variety of sources. Emittances for some materials were unavailable and were estimated from the values for similar materials. Values for drop properties are given in Table I. Variation of properties with temperature was neglected.

For calculations of drop fall in a helium atmosphere, thermophysical properties of the gas must also be known. Relevant properties include density, viscosity, thermal conductivity, and heat capacity.

For all calculations, we have assumed that the density of helium is given by the ideal gas law. This assumption is expected to be least accurate at the lowest temperature (293 K) and highest pressure (26 kPa) used in the calculations. Even under these conditions, the use of a van der Waals equation of state gives rise to a correction to the density of less than 0.025% [10]. The viscosity of helium was taken to be

$$\mu = \left[3.51068 \times 10^{-7} - 1.67969 \times 10^{-11}\left(\frac{T}{1\,\mathrm{K}}\right)\right]\left(\frac{T}{1\,\mathrm{K}}\right)^{0.71} \mathrm{Pa\,s} \quad (6)$$

where μ is the viscosity and T is the temperature. Division of temperature by 1 K is simply to remove units. Equation 6 was found to fit recommended values of viscosity [11] to within 0.36% over the temperature range 260–2500 K.

Data on the thermal conductivity of He from 260–2500 K were obtained from a handbook [12]. No single simple function was found that adequately described the data over this entire temperature range, so a cubic spline was fitted through the recommended values. The heat capacity of He at constant pressure was taken to be $2.5R$, where R is the gas constant, in accord with the kinetic theory of gases.

4. Results and discussion

A primary motivation for using a drop tube is that it provides an inexpensive way to replicate the containerless, low gravity processing that is available in space. It should be recognized, however, that although drop tubes do provide containerless processing, only experiments in vacuum provide microgravity (in the reference frame of the falling drop) for an appreciable period of time. In Fig. 1, we plot $(g - dU/dt)/g$, which is the retarding effect of the environment, as a function of time for two metals. The retarding effect is the sum of drag plus buoyancy. For a drop in a perfect vacuum, $\rho = 0$ and $(g - dU/dt)/g = 0$, while for a drop falling in an atmosphere at its (constant) terminal velocity, $(g - dU/dt)/g = 1$. (For the remainder of this paper, "drag plus buoyancy" will be referred to as "drag", since buoyancy is generally much smaller than drag.) In these calculations, each of the drops was taken to be at its melting point at the beginning of the fall. The gas temperature, T, was 293 K. Zero time corresponds to release of the drop from rest; the ends of the curves indicate the time of impact of the drop after falling 100 m. Various drop diameters and gas pressures were used. The lowest pressures (4 kPa for 3 mm and 8 kPa for 1 mm drops) are roughly those at which the effects of slip flow become significant, according to the classification scheme of Schaaf and Chambré [13]. With the exception of vacuum, the range of gas pressures considered has a substantial but not strong effect on acceleration of the drop. The effect of changing drop size from 3 to 1 mm at a fixed pressure is much stronger. It should also be observed that drag has a significant effect even at fairly short times for all non-zero gas pressures. Within 1 s, drag reduces the acceleration by more than $0.01g$ even in the case of the densest metal (Ni), largest drop (3 mm), and lowest gas pressure (4 kPa). Thus, while the drop is cooled in a containerless manner throughout its fall, the period that can be considered "low gravity" is fairly short if a gas coolant is used.

The period of time during which the drop experiences microgravity $((g - dU/dt)/g < 10^{-6})$ is extremely short. In Fig. 2, we show drag on a logarithmic scale; the value at zero time is due to buoyancy alone. The longest periods of microgravity are achieved with the denser metals at 4 kPa pressure of He and drop diameters of 3 mm, but, even for these cases, microgravity only lasts for about 60 μs. This is negligibly short, not even long enough for the drop to fall 20 nm. Note also that an experiment conducted in a drop tower in air at atmospheric pressure would fail to achieve microgravity by at least two orders of magnitude because of buoyancy alone.

In Fig. 3, we show temperature as a function of time. From this figure, we see that although drops cooled in a vacuum experience low gravity throughout the fall,

TABLE I Thermophysical properties of drop materials

Material	Al	Cu	Fe	Ni
Melting point (K)	933.52	1356.55	1808	1726
Surface tension ($N\,m^{-1}$)	0.914	1.360	1.872	1.778
Density ($kg\,m^{-3}$)	2380	7990	7010	7770
Emittance	0.15	0.15	0.29	0.29
Heat capacity (liquid) ($J\,kg^{-1}\,K^{-1}$)	1085.5	493.8	749.2	655.6
Heat capacity (solid) ($J\,kg^{-1}\,K^{-1}$)	1242.6	489.5	735.5	610.4
Enthalpy of fusion ($J\,kg^{-1}$)	398527	204772	289197	300079

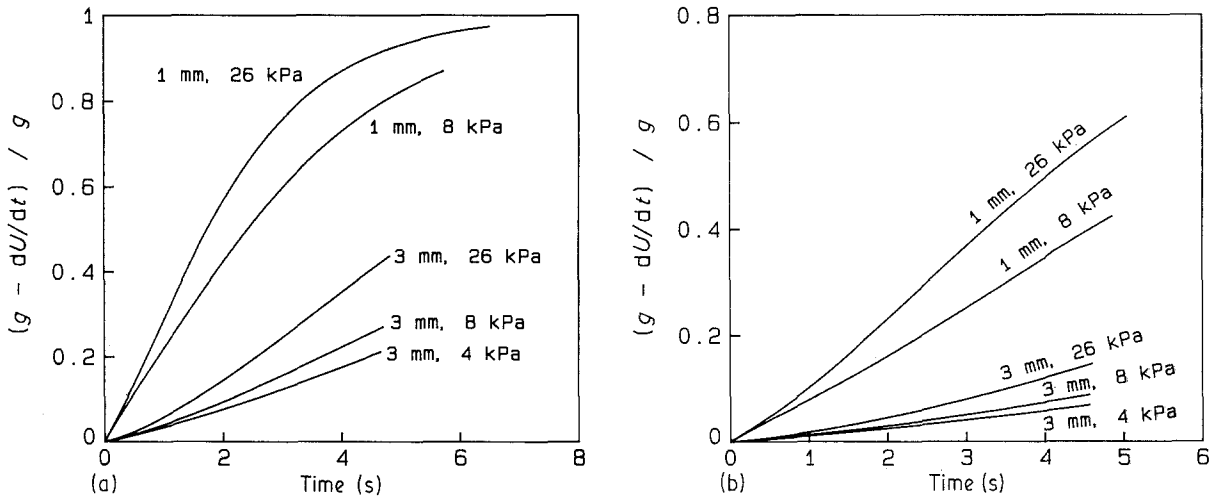

Figure 1 Drag $(g - dU/dt)/g$, as a function of time for supercooled liquid drops of specified diameter, falling in He at specified pressure (a) Al and (b) Cu. Plots for Fe and Ni are similar to those for Cu. Ends of curves correspond to impact of drops at the bottom of a 100 m drop tube.

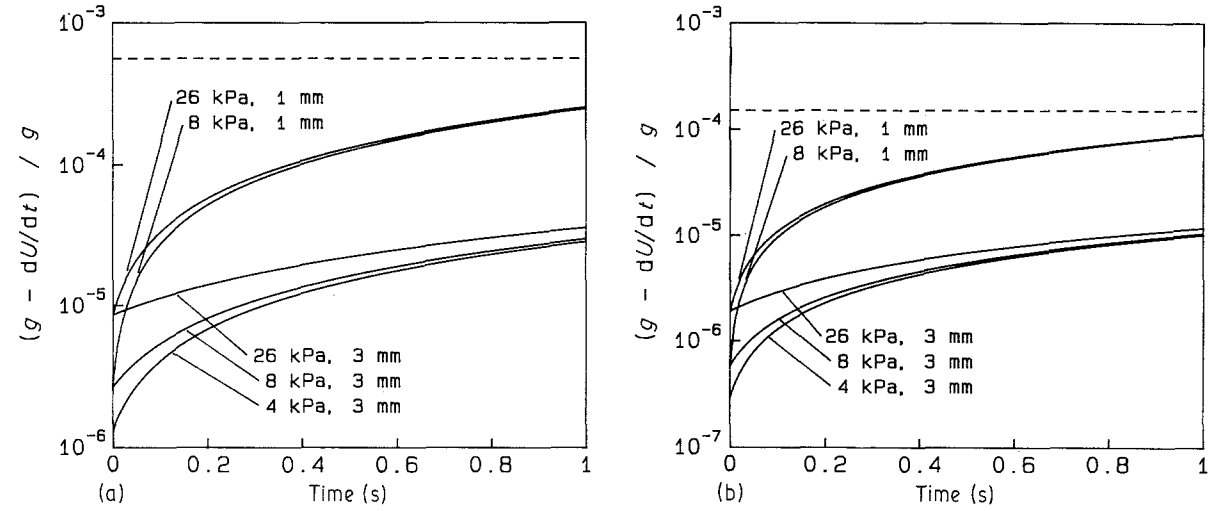

Figure 2 Drag $(g - dU/dt)/g$, as a function of time for supercooled liquid drops of specified diameter, falling in He at specified pressure (a) Al and (b) Cu. Dashed line shows effect of buoyancy alone for air at 101 kPa. Plots for Fe and Ni are similar to those for Cu.

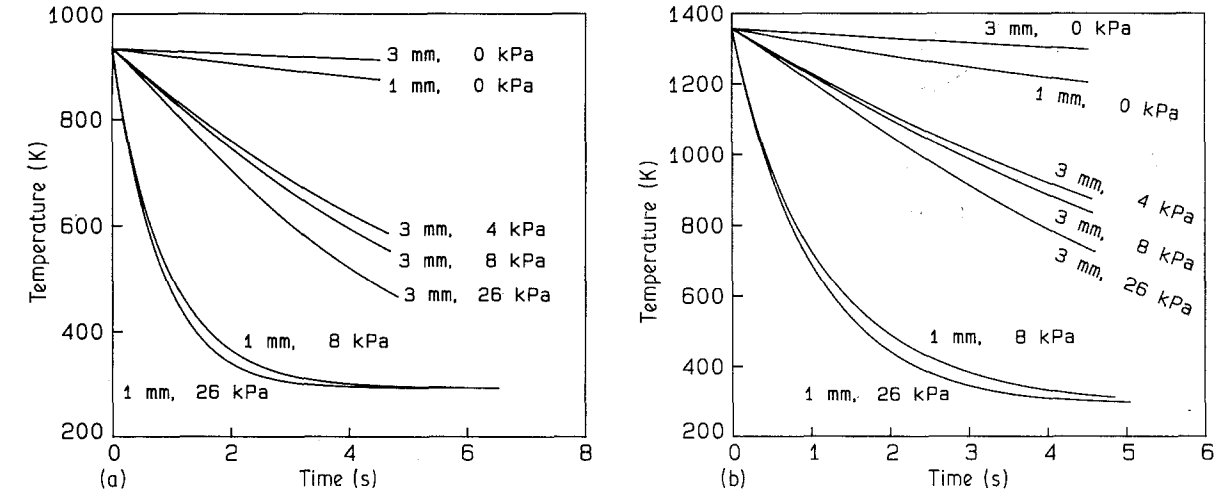

Figure 3 Temperature as a function of time for supercooled liquid drops of specified diameter falling in He at specified pressure (a) Al and (b) Cu. Plots for Fe and Ni are similar to those for Cu.

low gravity is obtained at the cost of a reduced cooling rate. Because of the strong dependence of radiation on temperature, the cooling rate in vacuum is smallest for Al, which has the lowest melting point, and largest for Fe, which has the highest melting point.

The data in Figs 1–3 cannot be used directly to compare the effectiveness of various combinations of drop size and gas pressure in cooling the drop with minimal drag, or in answering questions such as "which drop size and pressure (if any) will cool the

drop by 200 K while keeping the acceleration from drag less than $0.1g$?" Such problems can be addressed with plots like Fig. 4. Here we plot drag as a function of temperature. In these plots, the lowest curves correspond to those combinations of diameter and pressure that provide maximum cooling with minimum drag acceleration. Cooling a drop in vacuum eliminates drag, but the total amount of cooling is limited. At long times, low gas pressures are generally more effective than higher gas pressures for the same drop diameter. Surprisingly, however, the curves for non-zero gas pressure do not depend very strongly on either gas pressure or drop diameter. In several cases, the curves for 1 and 3 mm drops at the same gas pressure cross, although this is difficult to see in Fig. 4.

In the calculations above, it has been assumed that the drop remains liquid throughout its fall, regardless of the amount of supercooling. This has been the standard treatment in drop calculations. We have generalized our calculation to consider drops that partially or completely solidify in flight.

Solidification is handled by the following approach. The drop is assumed to cool in the liquid state until its temperature reaches a specified nucleation temperature. At this temperature, the drop instantaneously recalesces to the melting point, or, if the drop is hypercooled, it recalesces until solidification is complete. In the case of non-hypercooled drops, the temperature remains at the melting point until solidification is complete. This treatment involves two approximations: first, the assumption of instantaneousness requires that the solid–liquid interface move through the drop very rapidly, and, second, the use of a single drop temperature requires the assumption that the drop remains isothermal during recalescence.

Each of these approximations results in some inaccuracy, so we need to estimate the magnitude of the errors incurred. Let us first consider the assumption of an isothermal drop. Large thermal gradients will result as the solidification front moves through the drop. These will be removed by thermal diffusion. The characteristic time for removal of thermal gradients is given approximately by the equation $2(Dt)^{1/2} = d$ where D is the thermal diffusivity and t is the characteristic time. For 3 mm drops, the characteristic times vary from about 20 ms for Cu to about 110 ms for Fe. For 1 mm drops, the characteristic times will vary from about 2 to 12 ms. The model will therefore be inaccurate for approximately this length of time after recalescence begins. In Fig. 4, this would be reflected as a rounding of the sharp discontinuities that have been plotted. Because the time for thermal diffusion is short, the model is considered to be adequate for our present purposes.

In comparison, the assumption that the solid–liquid interface moves rapidly is relatively unimportant. For 3 mm drops, an interface speed of 0.15 m s^{-1} would suffice to cross a drop in the 20 ms required to produce thermal equilibrium in a Cu drop. Since the expected interface speeds for strongly supercooled drops are comparable to or higher than this [14], we conclude that the limitations on the model resulting from interface motion are comparable to or smaller than those imposed by thermal diffusion, at least for

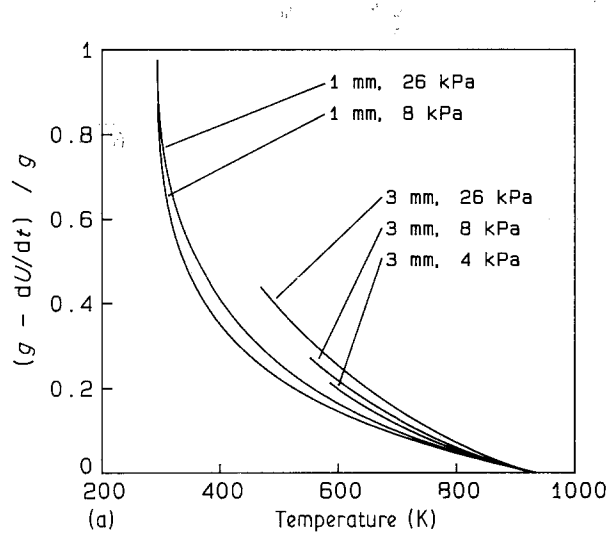

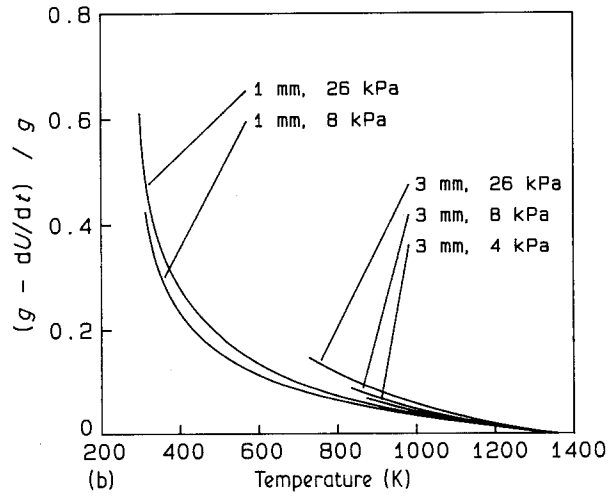

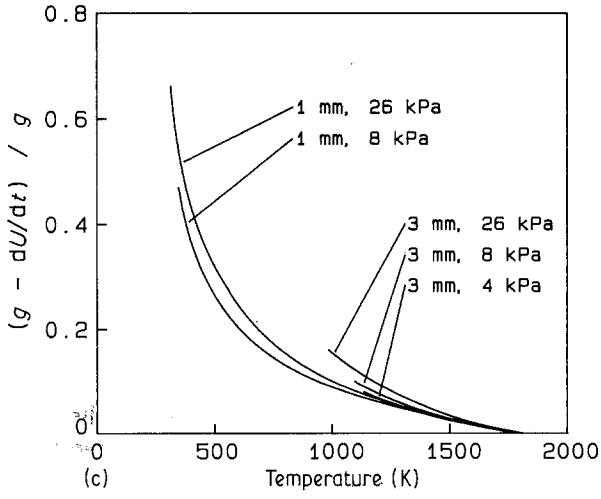

Figure 4 Drag $(g - dU/dt)/g$, as a function of temperature for supercooled liquid drops of specified diameter falling in He at specified pressure (a) Al, (b) Cu, (c) Fe. Plot for Ni is similar to that for Fe.

3 mm drops. Since the time to remove thermal gradients varies as the square of drop radius, while the time for the interface to cross the drop varies linearly with radius, interface motion becomes more important, relative to thermal diffusion, as drop size decreases. However, the time for removal of thermal gradients and the time for the interface to cross the drop are both shorter for smaller drops.

In Fig. 5, we show temperature as a function of time for 3 mm metal drops cooling in free fall. The atmosphere is He at 8 kPa pressure. All drops were started at their respective melting points, and nucleation temperatures of 0–400 K below the melting point were taken. In the case of aluminium with nucleation at 400 K below the melting point, the drop remains liquid until impact at the bottom of a 100 m drop tube; all other drops are completely solid on impact. For the conditions chosen here, hypercooling occurs only for Fe with 400 K supercooling.

The drops that begin to solidify at small supercoolings are completely solidified before those that begin to solidify only with larger supercoolings. This is expected, since a supercooled liquid drop has a lower temperature than a drop at the melting point, and therefore the supercooled drop loses heat less rapidly.

In Fig. 6, we plot drag as a function of the fraction of the drop that has solidified. Like Fig. 4, this can be used to determine the gravitational field felt by the drop during solidification. All curves start essentially at the origin. Curves for non-zero supercooling follow the y-axis as the liquid cools and drag builds up because of increasing speed. At the time of nucleation, part of the drop solidifies, and the flattish portion of the curve is crossed abruptly. The drag reaches at least $0.3\,m\,s^{-2}$ for all drops before solidification is complete, and it can be as large as $2\,m\,s^{-2}$ for Al drops.

5. Conclusions

A simple model for the cooling and solidification of a falling drop has been developed. The differential equations of motion and heat transfer have been solved for four elements under various conditions of gas pressure and drop diameter. Comparisons have been made of the effectiveness of these combinations of pressure and diameter in cooling the drop with minimal drag acceleration.

Recalescence of solidifying drops is modelled by assuming that the drop recalesces instantaneously. This model is used to determine the time necessary

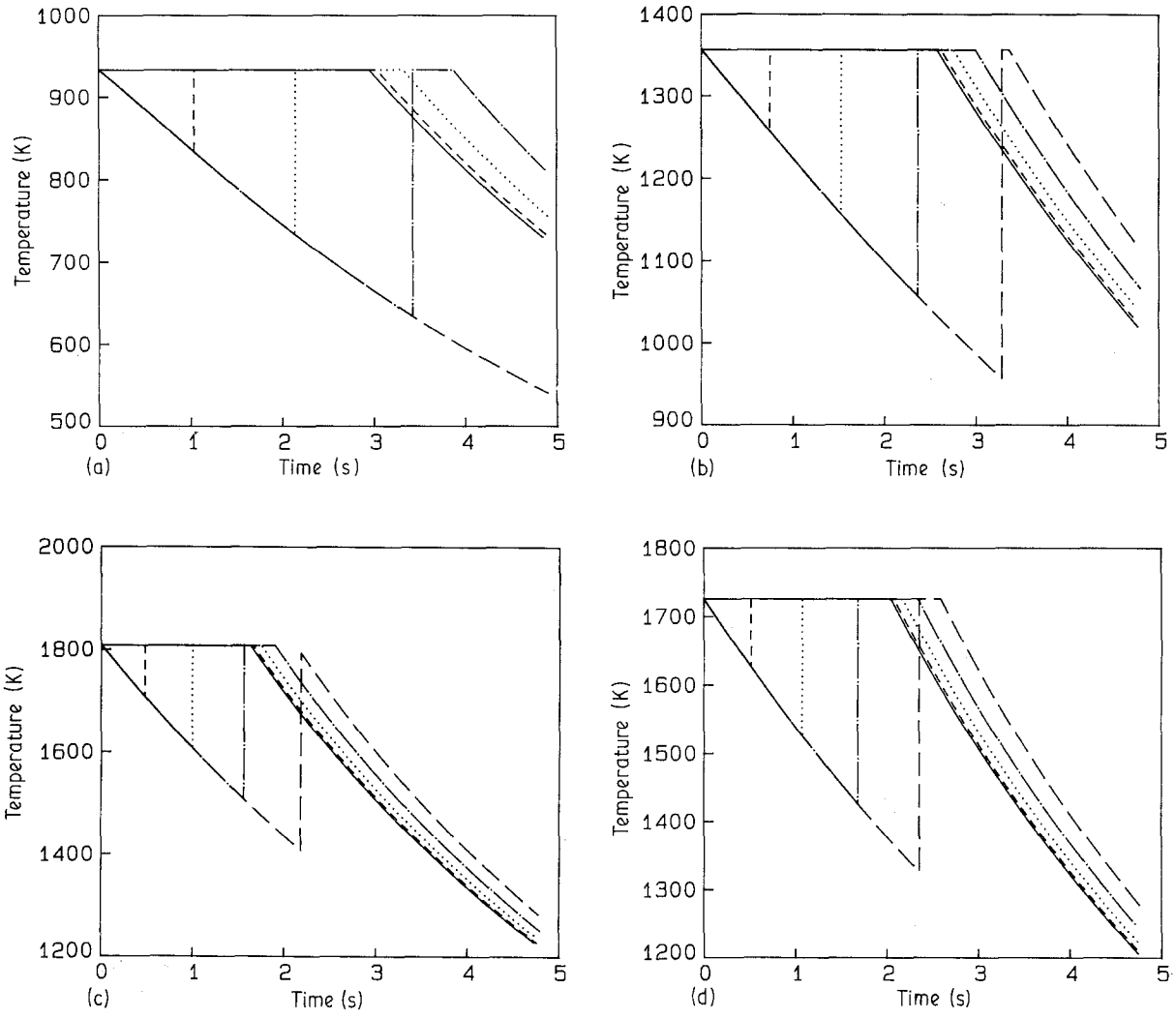

Figure 5 Temperature as a function of time for 3 mm drops falling in He at 8 kPa (a) Al, (b) Cu, (c) Fe and (d) Ni. Solid line corresponds to solidification beginning at 0 K supercooling, short dashed line to 100 K supercooling, dotted line to 200 K supercooling, dot-dashed line to 300 K supercooling, long dashed line to 400 K supercooling.

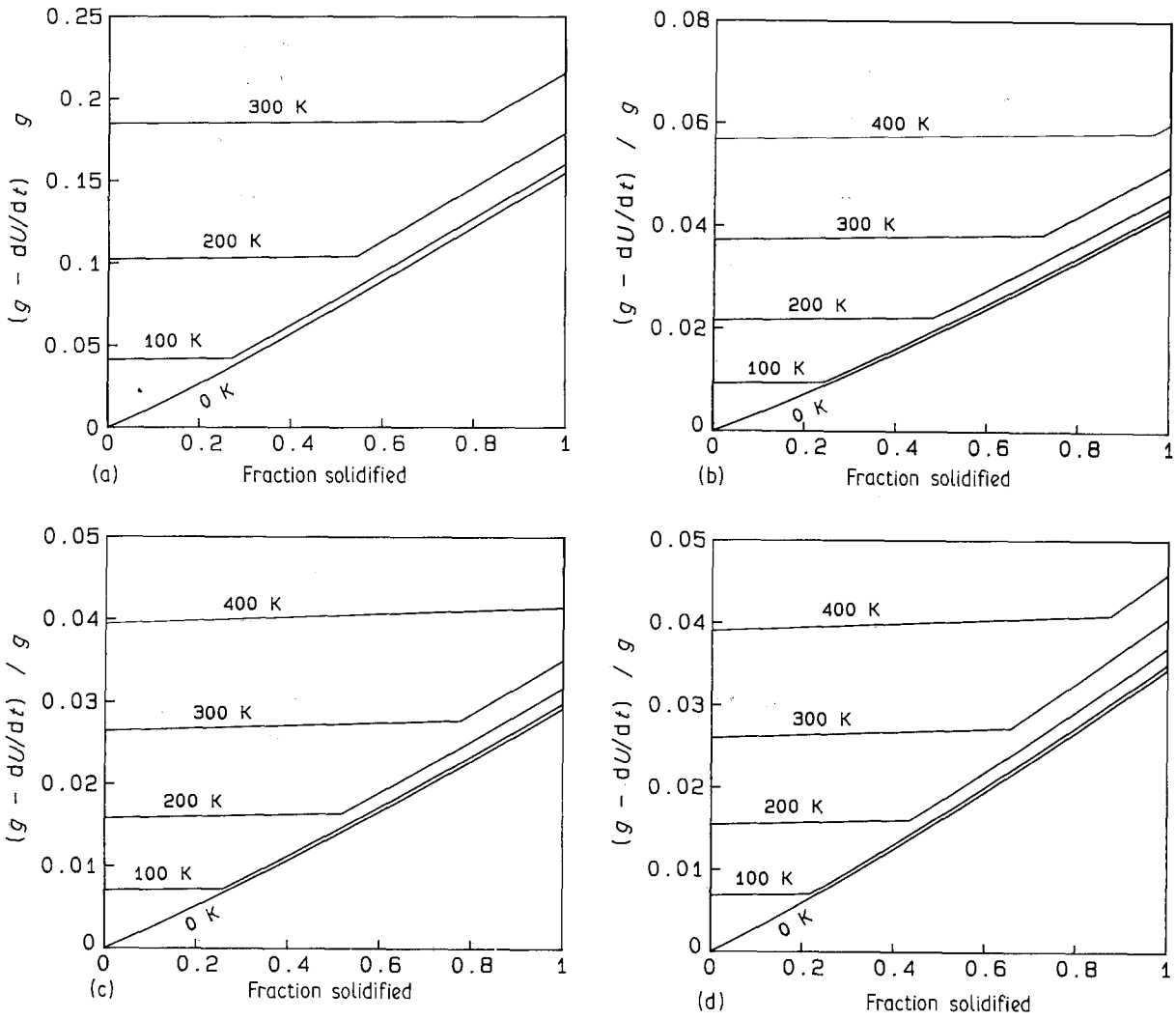

Figure 6 Drag $(g - dU/dt)/g$, as a function of fraction solidified for 3 mm drops falling in He at 8 kPa (a) Al, (b) Cu, (c) Fe and (d) Ni. Solidification begins at specified supercooling.

for complete solidification and the drag acceleration experienced by the drop during solidification.

Acknowledgement

Support of this work under NASA Contract NAS8–36608 is gratefully acknowledged.

References

1. L. L. LACY, M. B. ROBINSON and T. J. RATHZ, *J. Cryst. Growth* **51** (1981) 47.
2. R. J. BAYUZICK, N. D. EVANS, W. F. HOFMEISTER, K. R. JOHNSON and M. B. ROBINSON, *Adv. Space Res.* **4** (5) (1984) 85.
3. N. D. EVANS, W. F. HOFMEISTER, R. J. BAYUZICK and M. B. ROBINSON, *Metall. Trans.* **17A** (1986) 973.
4. W. F. HOFMEISTER, N. D. EVANS, R. J. BAYUZICK and M. B. ROBINSON, *ibid.* **17A** (1986) 1421.
5. M. B. ROBINSON, NASA Report NASA TM-78189 (1978).
6. J. K. McCOY, A. J. MARKWORTH, R. S. BRODKEY and E. W. COLLINGS, in "Materials Processing in the Reduced Gravity Environment of Space", edited by R. H. Doremus and P. C. Nordine (Materials Research Society, Pittsburgh, 1987) p. 163.
7. R. CLIFT, J. R. GRACE and M. E. WEBER, in "Bubbles, Drops, and Particles" (Academic, New York, 1978) p. 112.
8. G. DAHLQUIST and A. BJÖRCK, in "Numerical Methods" (Prentice-Hall, Englewood Cliffs, NJ, 1974) p. 346.
9. F. M. WHITE, in "Viscous Fluid Flow" (McGraw-Hill, New York, 1974).
10. R. C. WEAST (ed) in "CRC Handbook of Chemistry and Physics", 61st Edn (CRC Press, Boca Raton, Florida, 1980) p. D-194.
11. Y. S. TOULOUKIAN, S. C. SAXENA and P. HESTERMANS (eds), in "Thermophysical Properties of Matter" Vol. 11 (IFI/Plenum, New York, 1970) p. 18.
12. Y. S. TOULOUKIAN, P. E. LILEY and S. C. SAXENA (eds), in "Thermophysical Properties of Matter", Vol. 3 (IFI/Plenum, New York, 1970) p. 33.
13. S. A. SCHAAF and P. L. CHAMBRÉ, in Fundamentals of Gas Dynamics, Vol. 3, "High Speed Aerodynamics and Jet Propulsion", edited by H. W. Emmons (Princeton University, Princeton, 1958) p. 687.
14. P. PREDECKI, A. W. MULLENDORE and N. J. GRANT, *Trans. Metall. Soc. AIME* **223** (1965) 1581.

Received 8 October 1990
and accepted 20 March 1991